Application of reduced-order controller to turbulent flows for drag reduction

Keun H. Lee, Luca Cortelezzi,[a] John Kim,[b] and Jason Speyer
Department of Mechanical & Aerospace Engineering, University of California, Los Angeles, California 90095

(Received 18 April 2000; accepted 29 January 2001)

A reduced-order linear feedback controller is designed and applied to turbulent channel flow for drag reduction. From the linearized two-dimensional Navier–Stokes equations a distributed feedback controller, which produces blowing/suction at the wall based on the measured turbulent streamwise wall-shear stress, is derived using model reduction techniques and linear-quadratic-Gaussian/loop-transfer-recovery control synthesis. The quadratic cost criterion used for synthesis is composed of the streamwise wall-shear stress, which includes the control effort of blowing/suction. This distributed two-dimensional controller developed from a linear system theory is shown to reduce the skin friction by 10% in direct numerical simulations of a low-Reynolds number turbulent nonlinear channel flow. Spanwise shear-stress variation, not captured by the distributed two-dimensional controller, is suppressed by augmentation of a simple spanwise *ad hoc* control scheme. This augmented three-dimensional controller, which requires only the turbulent streamwise velocity gradient, results in a further reduction in the skin-friction drag. It is shown that the input power requirement is significantly less than the power saved by reduced drag. Other turbulence characteristics affected by these controllers are also discussed. © *2001 American Institute of Physics.* [DOI: 10.1063/1.1359420]

I. INTRODUCTION

Much attention has been paid to the drag reduction in turbulent boundary layers. Skin friction drag constitutes approximately 50%, 90%, and 100% of the total drag on commercial aircraft, underwater vehicles, and pipelines, respectively.[1] The decrease of skin friction, therefore, entails a substantial saving of operational cost for commercial aircraft and submarines. Recent reviews[1–3] summarize achievements and open questions in boundary layer control.

With the notion that near-wall streamwise vortices are responsible for high skin friction in turbulent boundary layers, Choi *et al.*[4] manipulated the near-wall turbulence by applying various wall actuations. They achieved a 20% skin-friction reduction in a turbulent channel flow by applying a wall transpiration equal and opposite to the wall–normal velocity component measured at $y^+ = 10$. This control is shown to effectively make the streamwise vortices weaker. However, it is not easily implementable since it is difficult to place sensors inside the flow field. Other attempts at weakening the near-wall streamwise vortices have been made by imposing spanwise oscillation of the wall[5] and using external body force.[6] These methods, however, require a large amount of input energy. A reduction in skin friction must be accompanied with the required input energy much less than the energy saved by the reduction.

A systematic approach, not relying on physical intuition, has been tried in the past. A suboptimal control, which determines the optimal control input by minimizing the cost functional for a short time interval, was successfully applied to the stochastic Burger's equation.[7] Bewley and Moin[8] extended the suboptimal control to a turbulent channel flow. This method, however, requires information about the whole flow field and excessive computation, so that it is impossible or at best extremely difficult to implement. It is necessary to develop a control scheme that utilizes easily measurable quantities.

Lee *et al.*[9] developed a neural network control algorithm that approximates the correlation between the wall-shear stresses and the wall actuation and then predicts the optimal wall actuation to produce the minimum value of skin friction. They also produced a simple control scheme from this neural network control, which determines the actuation as the sum of the weighted spanwise wall-shear stress, $\partial w/\partial y\,|_w$. Recently, Koumoutsakos[10] reported a substantial drag reduction obtained by applying a feedback control scheme based on the measurement and manipulation of the wall vorticity flux. Furthermore, he showed that the strength of unsteady mass transpiration actuators can be derived explicitly by inverting a system of equations.

Other systematic controls[11–17] have been developed by exploiting the tools recently developed in the control community.[18–21] Joshi *et al.*[11–13] and Bewley and Liu[14] developed an integral feedback controller, a linear quadratic (LQ) controller, and an $\mathcal{H}_\infty$ controller (worst-case controller) to successfully stabilize unstable disturbances in transitional flow. In particular, Cortelezzi and Speyer[15] introduced the multi-input–multi-output (MIMO) linear-quadratic-Gaussian (LQG)/loop-transfer-recovery (LTR) synthesis,[22] combined with model reduction techniques, for designing an optimal linear feedback controller. This controller successfully sup-

[a]Present address: Department of Mechanical Engineering, McGill University, Montreal, Quebec, Canada; electronic mail: crtlz@ametista.mecheng.mcgill.ca
[b]Author to whom correspondence should be addressed. Telephone: (310) 825-4393; fax: (310) 206-4830; electronic mail: jkim@seas.ucla.edu

pressed near-wall disturbances, thus preventing a transition in two-dimensional laminar channel flows. This reduced-order controller[16] was applied to two-dimensional nonlinear transitional flows, illustrating that the controller designed from the linear model works remarkably well in nonlinear flows.

Our purpose in the present study is to develop a realistic robust optimal controller that systematically determines the wall actuation, in the form of blowing and suction at the wall, relying only on a measured streamwise velocity gradient to reduce skin friction in a fully developed turbulent channel flow. A dynamic representation of the flow field is required for controller design. Due to the complexity and nonlinearity of the Navier–Stokes equations, it is difficult to derive model-based controllers. Therefore, the linearized Navier–Stokes equations for Poiseuille flow are used as an approximation of the flow field and form the basis of system modeling. Several investigators (e.g., Farrel and Ioannou,[23] Kim and Lim,[24] to name a few) have shown that linearized models have a direct relevance to turbulent flows. A reduced-order controller has been designed based on this model and applied to linear and nonlinear transitional flows.[15–17] Encouraged by these results, in this paper we apply this distributed two-dimensional controller to a direct numerical simulation of turbulent channel flow at a low Reynolds number. We then augment our two-dimensional distributed controller by including an *ad hoc* control scheme to attenuate the residual disturbances in the spanwise direction.

In Sec. II, we derive the state-space equations from the linearized two-dimensional Navier–Stokes equations. In Sec. III, we reduce the order of the state-space equations and derive a reduced-order two-dimensional controller by using LQG/LTR synthesis. In Sec. IV, we construct and apply the distributed two-dimensional controller based on the linearized Navier–Stokes equations to a fully developed turbulent channel flow at $\mathrm{Re}_\tau = 100$, where Re_τ is the Reynolds number based on the wall-shear velocity, u_τ, and the half-channel height, h. In Sec. V, this distributed two-dimensional controller augmented with a simple *ad hoc* control scheme is applied to the same flow. In Sec. VI, we present turbulence statistics associated with the controlled flows followed by conclusions in Sec. VII.

In this paper, we use (u,v,w) to represent the velocity components in the streamwise (x), wall–normal (y), and spanwise (z) directions, respectively.

II. THE STATE-SPACE EQUATIONS

One of the goals in the present study is to reduce the size of the controller. A controller with a large number of states is of no practical interest in engineering applications because of the amount of hardware and computer power necessary to compute a real-time control law. Consequently, it is crucial to reduce the order of the controller.

Figure 1 shows the configuration of the turbulent channel flow equipped with the controller tested for our study. Low-order controllers are usually preferred to high-order one because of the lower cost of hardware construction as well as the less computation time necessary to provide the control

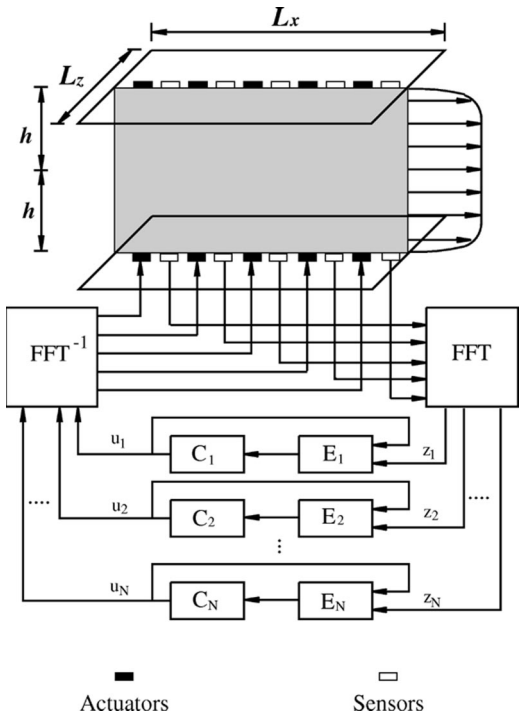

FIG. 1. Schematic representation of turbulent channel flow equipped with sensors and actuators distributed in the streamwise direction in each z plane.

input. Hence, we slice the channel with xy planes equally spaced in the z direction in order to reduce the order of the controller. We then construct the distributed two-dimensional controller by applying the two-dimensional controller developed from the linearized two-dimensional Navier–Stokes equations[15] to each plane. It is shown[16] that the two-dimensional controller is effectively able to reduce the skin-friction drag of the finite-amplitude disturbances in a two-dimensional channel flow.

We follow the same derivation of the state-space equation as given in Cortelezzi *et al.*[16] We give a brief outline here for completeness; the interested reader is referred to Cortelezzi *et al.*[16] for details. The wall transpiration is applied to both top and bottom walls in a fully developed turbulent channel flow. For simplicity, though, we derive the state-space equations assuming that blowing and suction is applied only at the bottom wall. The application of blowing and suction to both walls is a trivial extension.

We consider two-dimensional incompressible Poiseuille flow in a periodic channel of streamwise length, L_x, and channel height, $2h$. The undisturbed velocity field has a parabolic profile with centerline velocity U_c. The linearized two-dimensional Navier–Stokes equations can be written in terms of the perturbation streamfunction, ψ,

$$(\partial_t + U\partial_x)\Delta\psi - U''\psi_x = \mathrm{Re}^{-1}\Delta\Delta\psi, \tag{1}$$

where all variables are normalized with U_c and h and $\mathrm{Re} = U_c h/\nu$ is the Reynolds number.

To suppress perturbations evolving within the bottom boundary layer, we apply blowing and suction at the bottom wall (see Fig. 1). For simplicity, we assume that the actuators are continuously distributed. The corresponding boundary conditions are

$$\psi_x|_{y=-1} = -v_w(x,t), \quad \psi_y|_{y=\pm 1} = \psi|_{y=1} = 0, \tag{2}$$

where the control function v_w indicates blowing and suction at the bottom wall. We impose the wall transpiration of zero net mass flux.

To detect the near-wall disturbances, we measure the gradient of the streamwise disturbance velocity at given point $x = x_i$ along the bottom wall (see Fig. 1),

$$z(x_i,t) = \psi_{yy}|_{y=-1}. \tag{3}$$

In other words, we measure the first term of the disturbance wall-shear stress, $\tau_{yx} = \mathrm{Re}^{-1}(\psi_{yy} - \psi_{xx})|_{y=-1}$. The second term of the wall-shear stress is zero in the uncontrolled case and is known in the controlled case.

We define a performance index $\tilde{\mathcal{J}}$, or cost criterion, to design a controller for the LQG ($\mathcal{H}_2$) problem. Since we are interested in suppressing the disturbance wall-shear stress, τ_{yx}, we define

$$\tilde{\mathcal{J}} = \lim_{t_f \to \infty} \int_t^{t_f} \int_0^L (\psi_{yy}^2 + \psi_{xx}^2)|_{y=-1} dx dt. \tag{4}$$

The integrand represents the cost of the disturbance wall-shear stress, τ_{yx}, being different from zero. Moreover, the integrand implicitly accounts for the cost of implementing the control itself. There are two reasons to minimize the cost of the control. In any engineering application the energy available to drive the controller is limited, and a large control action may drive the system away from the region where the linear model is valid.

By using the same procedure described in Cortelezzi *et al.*,[16] Eqs. (1)–(3) are converted into the state-space equations:

$$\frac{d\mathbf{x}}{dt} = \mathbf{A}\mathbf{x} + \mathbf{B}\mathbf{u}, \quad \mathbf{z} = \mathbf{C}\mathbf{x} + \mathbf{D}\mathbf{u}, \tag{5}$$

with the initial condition $\mathbf{x(0)} = \mathbf{x_0}$, where $\mathbf{x}$ is the internal state vector, $\mathbf{u}$ is the control vector, $\mathbf{z}$ is the measurement vector. Matrices **A,B,C** contain the dynamics of the two-dimensional plane Poiseuille flow, actuators, and sensors, respectively. Matrix **D** contains the coupling between sensors and actuators. The cost criterion, Eq. (4), becomes

$$\tilde{\mathcal{J}} = \lim_{t_f \to \infty} \int_t^{t_f} [\mathbf{z}^T\mathbf{z} + \mathbf{u}^T\mathbf{F}^T\mathbf{F}\mathbf{u}] dt, \tag{6}$$

where the superscript T denotes a transposed quantity. The matrix $\mathbf{F}$ is obtained by spectrally decomposing the last term in the cost criterion, Eq. (4).

The advantage of the present formulation is that the whole problem decouples with respect to the wave number when Eqs. (5) and (6) are transformed into Fourier space in the streamwise direction. All matrices in Eqs. (5) and (6) are block diagonal, which allows the above state-space system into equivalent N state-space subsystems.[25] For a given wave number, α, the state-space subsystem equations are

$$\frac{d\mathbf{x}_\alpha}{dt} = \mathbf{A}_\alpha\mathbf{x}_\alpha + \mathbf{B}_\alpha\mathbf{u}_\alpha, \quad \mathbf{z}_\alpha = \mathbf{C}_\alpha\mathbf{x}_\alpha + \mathbf{D}_\alpha\mathbf{u}_\alpha, \tag{7}$$

with the initial condition $\mathbf{x}_\alpha(0) = \mathbf{x}_{\alpha 0}$. It can be shown that the cost criterion, Eq. (6), also decouples with respect to the wave number (otherwise the wave number decoupling is not possible while the system itself is decoupled), and we obtain N performance indexes. For a given wave number, α, the cost criterion is defined as

$$\tilde{\mathcal{J}}_\alpha = \lim_{t_f \to \infty} \mathcal{J}_\alpha = \lim_{t_f \to \infty} \int_t^{t_f} [\mathbf{z}_\alpha^T\mathbf{z}_\alpha + \mathbf{u}_\alpha^T\mathbf{F}_\alpha^T\mathbf{F}_\alpha\mathbf{u}_\alpha] dt. \tag{8}$$

Consequently, the design of a two-dimensional controller for the system, Eq. (5), with a specified cost criterion, Eq. (6), has been reduced to the independent design of N single-wave number controllers for the subsystems, Eq. (7), along with Eq. (8).

III. MODEL REDUCTION AND CONTROLLER DESIGN

In this section we derive a lower-order two-dimensional controller in two steps.[15] First, we construct a lower-order model of Eq. (7), and subsequently, design a single-wave number controller for the reduced-order model. To obtain a lower-order model, we transform Eq. (7) into a Jordan canonical form. The matrices $\hat{\mathbf{A}}_\alpha, \hat{\mathbf{B}}_\alpha, \hat{\mathbf{C}}_\alpha, \mathbf{D}_\alpha$ that describe the dynamics of the reduced-order model are obtained from the matrices, $\mathbf{A}_\alpha, \mathbf{B}_\alpha, \mathbf{C}_\alpha, \mathbf{D}_\alpha$ in the Jordan canonical form by retaining rows and columns corresponding to equally well controllable and observable states. The overcaret denotes the quantities associated with the reduced-order model.

Although a rigorous mathematical framework for the design of disturbance attenuation ($\mathcal{H}_\infty$) linear controllers is provided by the control synthesis theory,[18,19] for this study LQG($\mathcal{H}_2$) synthesis is preferred. A brief review will be given in a self-contained manner to provide the necessary governing equations for closed-loop stability analysis.[20]

The LQG problem for each wave number α is formulated as a stochastic optimal control problem described by equations

$$\dot{\hat{\mathbf{x}}}_\alpha = \hat{\mathbf{A}}_\alpha\hat{\mathbf{x}}_\alpha + \hat{\mathbf{B}}_\alpha\mathbf{u}_\alpha + \mathbf{\Gamma}_\alpha\mathbf{w}_\alpha, \tag{9}$$

$$\hat{\mathbf{z}}_\alpha = \hat{\mathbf{C}}_\alpha\hat{\mathbf{x}}_\alpha + \mathbf{D}_\alpha\mathbf{u}_\alpha + \mathbf{v}_\alpha, \tag{10}$$

where $\mathbf{\Gamma}_\alpha$ is an input matrix, $\mathbf{w}_\alpha$ and $\mathbf{v}_\alpha$ are both white noise processes with zero means and autocorrelation functions,

$$\begin{aligned} E[\mathbf{w}_\alpha(t)\mathbf{w}_\alpha^T(\tau)] &= \mathbf{W}_\alpha\delta(t-\tau), \\ E[\mathbf{v}_\alpha(t)\mathbf{v}_\alpha^T(\tau)] &= \mathbf{V}_\alpha\delta(t-\tau), \end{aligned} \tag{11}$$

where $E[\cdot]$ is the expectation operator averaging over all underlying random variables and $\delta(t-\tau)$ is the delta function. Note that $\mathbf{W}_\alpha$ and $\mathbf{V}_\alpha$, the power spectral densities, will be chosen here as design parameters to enhance system performance. An additional comment on the controller design process will be given at the end of this section.

The LQG controller is determined by finding the control action $\mathbf{u}_\alpha(Z_t)$, where $Z_t = \{z(\tau); 0 \leqslant \tau \leqslant t\}$ is the measurement history, which minimizes the cost criterion,

$$J_\alpha = \lim_{t_f\to\infty} \frac{1}{t_f - t} \times E\left(\int_t^{t_f} (\hat{\mathbf{x}}_\alpha^T \mathbf{Q}_\alpha \hat{\mathbf{x}}_\alpha + 2\hat{\mathbf{x}}_\alpha^T \mathbf{N}_\alpha \mathbf{u}_\alpha + \mathbf{u}_\alpha^T \mathbf{R}_\alpha \mathbf{u}_\alpha) d\tau \right), \quad (12)$$

subject to the stochastic dynamics system model equations Eqs. (10)–(11). Note that, from Eqs. (7)–(8), $\mathbf{Q}_\alpha = \hat{\mathbf{C}}_\alpha^T \hat{\mathbf{C}}_\alpha$, $\mathbf{N}_\alpha = \hat{\mathbf{C}}_\alpha^T \mathbf{D}_\alpha$, and $\mathbf{R}_\alpha = \mathbf{D}_\alpha^T \mathbf{D}_\alpha + \mathbf{F}_\alpha^T \mathbf{F}_\alpha$. The division by $(t_f - t)$ ensures that the cost criterion remains finite in the presence of uncertainties in the infinite-time problem $(t_f \to \infty)$. Note that Eq. (12) can include Eq. (8), where

$$J_\alpha = \lim_{t_f\to\infty} \frac{1}{t_f - t} E[\mathcal{J}_\alpha], \quad (13)$$

and the limit in Eq. (8) is explicitly denoted in Eq. (13). Note that even though the time interval is infinite, the time response is still measured by the eigenvalues of the closed-loop system. We consider the infinite-time problem with time-invariant dynamics because the controller gains become constants.

By nesting the conditional expectation with respect to Z_t within the unconditional expectation of Eq. (13), i.e., $E[\mathcal{J}_\alpha] = E[E[\mathcal{J}_\alpha / Z_t]]$, where $E[\cdot / Z_t]$ denotes the expectation $(\cdot)$ conditioned on Z_t, the cost criterion can be written as

$$J_\alpha = \lim_{t_f\to\infty} \frac{1}{t_f - t} \times E\left(\int_t^{t_f} [\tilde{\mathbf{x}}_\alpha^T \mathbf{Q}_\alpha \tilde{\mathbf{x}}_\alpha + 2\tilde{\mathbf{x}}_\alpha^T \mathbf{N}_\alpha \mathbf{u}_\alpha + \mathbf{u}_\alpha^T \mathbf{R}_\alpha \mathbf{u}_\alpha + \mathrm{tr}(\mathbf{P}_\alpha)] d\tau \right), \quad (14)$$

where $\tilde{\mathbf{x}}_\alpha = E[\hat{\mathbf{x}}_\alpha / Z_t]$ is the conditional mean estimate of the state $\hat{\mathbf{x}}$ and $\mathbf{P}_\alpha$ is the conditional error variance. This cost criterion is now minimized subject to the estimation equations discussed below. Note that $\mathbf{P}_\alpha$ does not depend on the control [see Eq. (18) below] and, therefore, does not enter into the optimization process.

The solution to the regulator problem[20] is a compensator composed of a state reconstruction process, known here as a filter (in the no-noise case it is known as an observer) in cascade with a controller (see Fig. 1, where E_i is the estimator and C_i is the controller). The state estimate (conditional mean) $\tilde{\mathbf{x}}_\alpha$ is governed by the so-called Kalman filter as

$$\begin{aligned} \dot{\tilde{\mathbf{x}}}_\alpha &= \hat{\mathbf{A}}_\alpha \tilde{\mathbf{x}}_\alpha + \hat{\mathbf{B}}_\alpha \mathbf{u}_\alpha + \hat{\mathbf{L}}_\alpha \boldsymbol{\nu}_\alpha, \\ \boldsymbol{\nu}_\alpha &= \hat{\mathbf{z}}_\alpha - \tilde{\mathbf{z}}_\alpha = \hat{\mathbf{C}}_\alpha (\hat{\mathbf{x}}_\alpha - \tilde{\mathbf{x}}_\alpha) + \mathbf{v}_\alpha. \end{aligned} \quad (15)$$

If the reduced-order system were the actual system, then $\boldsymbol{\nu}_\alpha$ in Eq. (15) is correct. When the actual system is considered and the filter is implemented based on the reduced-state space, $\mathbf{z}$ rather than $\hat{\mathbf{z}}$ is the measurement and the filter residual becomes

$$\boldsymbol{\nu}_\alpha = \mathbf{z}_\alpha - \hat{\mathbf{C}}_\alpha \tilde{\mathbf{x}}_\alpha - \mathbf{D}_\alpha \mathbf{u}_\alpha. \quad (16)$$

The Kalman gain matrix $\mathbf{L}_\alpha$, constructed to trade the accuracy of the new measurements against the accuracy of the state propagated from the system dynamics, is given by

$$\hat{\mathbf{L}}_\alpha = \mathbf{P}_\alpha \hat{\mathbf{C}}_\alpha^T \mathbf{V}_\alpha^{-1}, \quad (17)$$

where $\mathbf{P}_\alpha$ is the error variance in the statistical problem.

In the infinite-time stationary formulation, the error $\mathbf{P}_\alpha$ is the solution to the algebraic Riccati equation (ARE),

$$\hat{\mathbf{A}}_\alpha \mathbf{P}_\alpha + \mathbf{P}_\alpha \hat{\mathbf{A}}_\alpha^T + \boldsymbol{\Gamma}_\alpha \mathbf{W}_\alpha \boldsymbol{\Gamma}_\alpha^T - \mathbf{P}_\alpha \hat{\mathbf{C}}_\alpha^T \mathbf{V}_\alpha^{-1} \hat{\mathbf{C}}_\alpha \mathbf{P}_\alpha = 0. \quad (18)$$

If the system is $(\hat{\mathbf{A}}_\alpha, \hat{\mathbf{C}}_\alpha)$ observable and $(\hat{\mathbf{A}}_\alpha, \hat{\mathbf{B}}_\alpha)$ controllable, then $\mathbf{P}_\alpha$ is positive definite. Under these assumptions, it can be shown that the difference between the internal state $\hat{\mathbf{x}}_\alpha$ and the estimate state $\tilde{\mathbf{x}}_\alpha$, i.e., the error,

$$\mathbf{e}_\alpha = \hat{\mathbf{x}}_\alpha - \tilde{\mathbf{x}}_\alpha, \quad (19)$$

goes to zero as time goes to infinity. In other words, the evolution equation,

$$\dot{\mathbf{e}}_\alpha = \mathbf{A}_f \mathbf{e} + \hat{\mathbf{L}}_\alpha \boldsymbol{\nu} + \boldsymbol{\Gamma}_\alpha \mathbf{w}, \quad (20)$$

is stable, i.e., all the eigenvalues of the matrix,

$$\mathbf{A}_f = \hat{\mathbf{A}}_\alpha - \hat{\mathbf{L}}_\alpha \hat{\mathbf{C}}_\alpha, \quad (21)$$

have a negative real part.

Minimizing the infinite-time cost function J, Eq. (14) subject to Eq. (15) yields the following control law:

$$\mathbf{u}_\alpha = -\hat{\mathbf{K}}_\alpha \tilde{\mathbf{x}}_\alpha, \quad (22)$$

where

$$\hat{\mathbf{K}}_\alpha = \mathbf{R}_\alpha^{-1} (\hat{\mathbf{B}}_\alpha^T \mathbf{S}_\alpha + \mathbf{N}_\alpha), \quad (23)$$

and $\mathbf{S}_\alpha$ is the solution of the algebraic Riccati equation (ARE),

$$\hat{\mathbf{A}}_\alpha \mathbf{S}_\alpha + \mathbf{S}_\alpha \hat{\mathbf{A}}_\alpha^T + \mathbf{Q}_\alpha - (\mathbf{S}_\alpha \mathbf{B}_\alpha + \mathbf{N}_\alpha) \mathbf{R}_\alpha^{-1} (\mathbf{B}_\alpha^T \mathbf{S}_\alpha + \mathbf{N}_\alpha^T) = 0. \quad (24)$$

It should be remarked that the control gain matrix $\hat{\mathbf{K}}_\alpha$ is determined from functions only of the known dynamics coefficients $(\hat{\mathbf{A}}_\alpha, \hat{\mathbf{B}}_\alpha)$ and the weighting in the cost criterion $(\mathbf{Q}_\alpha, \mathbf{R}_\alpha)$, and not the statistic of the input $(\mathbf{V}_\alpha, \mathbf{W}_\alpha)$. Consequently, $\hat{\mathbf{K}}_\alpha$ is determined from a performance index as Eq. (12), independent of the stochastic inputs. If $(\hat{\mathbf{A}}_\alpha, \hat{\mathbf{B}}_\alpha)$ is controllable and $(\hat{\mathbf{A}}_\alpha, \mathbf{Q}_\alpha^{1/2})$ observable, then the loop coefficient matrix,

$$\mathbf{A}_c = \hat{\mathbf{A}}_\alpha - \hat{\mathbf{K}}_\alpha \hat{\mathbf{B}}_\alpha, \quad (25)$$

is stable and $\mathbf{S}_\alpha$ is positive definite. The controllable and observable conditions can be weakened to stabilizable and detectable.[21]

When we combine the estimator and the regulator together, the dynamic system composed of the controlled process and filter becomes

$$\begin{pmatrix} \dot{\mathbf{e}}_\alpha \\ \dot{\tilde{\mathbf{x}}}_\alpha \end{pmatrix} = \begin{bmatrix} \mathbf{A}_f & \mathbf{0} \\ \hat{\mathbf{L}}_\alpha \hat{\mathbf{C}}_\alpha & \mathbf{A}_c \end{bmatrix} \begin{pmatrix} \mathbf{e}_\alpha \\ \tilde{\mathbf{x}}_\alpha \end{pmatrix} + \begin{pmatrix} \hat{\mathbf{L}}_\alpha \mathbf{v}_\alpha + \boldsymbol{\Gamma}_\alpha \mathbf{w}_\alpha \\ \hat{\mathbf{L}}_\alpha \mathbf{v}_\alpha \end{pmatrix}. \quad (26)$$

Note that any choice of two between $\mathbf{e}$, $\hat{\mathbf{x}}_\alpha$, and $\tilde{\mathbf{x}}_\alpha$ produce the same dynamics because they are algebraically related by

Eq. (19). Under the above controllability and observability assumptions, $\mathbf{A}_f$ and $\mathbf{A}_c$ have only stable eigenvalues if optimal gains $\hat{\mathbf{L}}_\alpha$ and $\hat{\mathbf{K}}_\alpha$ of Eqs. (17) and (23) are used. If the actual linear system is used, then $\mathbf{x}_\alpha$ and the reduced-order state estimate $\tilde{\mathbf{x}}_\alpha$ are used to form the closed-loop dynamic system rather than that given in Eq. (26). The eigenvalues of the dynamical matrix now dictate the system stability and will differ from the ideal case of Eq. (26).

The parameters used in our LQG design are now addressed. Since the power spectral density is not known, for simplicity of the design we consider $\mathbf{V}_\alpha$ and $\mathbf{W}_\alpha$ to be of the form $\mathbf{V}_\alpha=\beta\mathbf{I}$ and $\mathbf{W}_\alpha=\rho\mathbf{I}$, where β and ρ are scalar and $\mathbf{I}$ is an identity matrix. Only the ratio of β and ρ is important. Furthermore, by choosing $\mathbf{\Gamma}_\alpha=\hat{\mathbf{B}}_\alpha$, loop-transfer recovery (LTR) of the LQG controller to full-state feedback[18] guarantees that robust performance occurs when the process noise power spectral density goes to infinity, i.e., $\rho\to\infty$, provided there exists no nonminimal-phase zero in the plant. In our case, there are no nonminimal-phase zeros and robust performance means approximately obtaining 60° of phase margin and 6 db of the gain margin. Note that the choice of $\mathbf{\Gamma}_\alpha=\hat{\mathbf{B}}_\alpha$ implies that the noise is generated along the wall as is the control and could be interpreted as due to wall roughness. Furthermore, the values of ρ and β were determined by tuning the controller in the presence of turbulent flow. The degree of loop transfer recovery varied from controller to controller.

As described above using LQG/LTR assumes that the uncertainty is at the wall and effects the dynamics in the same way as the control. Since the system has the same controllability with respect to both the control and disturbances, state-space reduction for controller design was straightforward. This is in contrast to $\mathcal{H}_\infty$ control used by Bewley and Liu,[14] where uncertainty is assumed uniformly throughout the channel. Since controllability of the disturbances is different from that of the control, model reduction may not be straightforward. Furthermore, robustness in terms of traditional measures of the gain and phase margin in control engineering are also obtained by using LQG/LTR. For these reasons LQG/LTR is used for the present study instead of the unstructured uncertainty $\mathcal{H}_\infty$ controllers.

Figure 1 links the mathematical formulation to its computational implementation by summarizing in a block diagram the control strategy described above. The two-dimensional distributed controller can be programmed in a computer routine whose input is a matrix containing the gradients of the streamwise velocity component and whose output is a matrix containing the blowing and suction at the wall. Each column of the measurement matrices contains the gradients of the streamwise velocity component along the wall at a given spanwise location. Each column is processed in parallel by a fast Fourier transform (FFT) and converted into $\mathbf{z}_\alpha$'s. Each single-wave number controller, Eqs. (9)–(10), is integrated in time by, for example, a third-order low-storage Runge–Kutta scheme. The $\mathbf{u}_\alpha$'s are computed in parallel. An inverse FFT converts $\mathbf{u}_\alpha$'s into the columns of the matrix containing the blowing and suction at the wall along the streamwise direction. This routine can be embedded in any Navier–Stokes solver able to handle time-dependent boundary conditions for the control of three-dimensional channel flows.

Figure 1 also provides the basic architecture for the potential implementation of the present distributed two-dimensional controller in practical engineering applications. For instance, the gradients of the streamwise velocity component can be measured by microelectromechanical-systems (MEMS) hot-film sensors.[26] For each xy plane, analog-to-digital converters (A/D) and digital signal processors (DSP) convert the measured gradients into $\mathbf{z}_\alpha$'s. Each single-wave number controller, Eqs. (9)–(10), is replaced by a microprocessor, and parallel computation produces $\mathbf{u}_\alpha$'s. A DSP and a digital-to-analog converter (D/A) produce the actuating signal in each xy plane. A variety of actuators, such as synthetic jets, microbubble actuators, and thermal actuators, can mimic small-amplitude blowing and suction at the wall.[26]

Although the structure of this compensator is simplified by the parallel computation (for all spanwise directions), it does require processing of all the sensor measurements (for all streamwise directions). The controller is essentially centralized because all information is used and the actuators are activated spatially over the assumed channel. Controllers based explicitly on the spatial distribution of the control, suggested by Bamieh *et al.*,[27] show that there is a spatial decay rate. Our controller can be constructed to represent a discrete form of their controller and given the spatial decay rate for our configuration, i.e., the size of the channel could be chosen consistent with that decay rate. Nevertheless, our representation allows a significant decrease in on-line computation by identifying the Fourier modes and the number of states associated with those modes that best reduce turbulence as discussed in the next section.

IV. PERFORMANCE OF A TWO-DIMENSIONAL CONTROLLER

For the purpose of testing the performance of a controller, we performed direct numerical simulations of a turbulent channel flow at $\mathrm{Re}_\tau=100$. A spectral code was used with a computational domain of $(4\pi,2,4\pi/3)$ and a grid resolution of (32,65,32) in the (x,y,z) directions. The numerical technique used in this study is essentially the same as that of Kim *et al.*[28] except that the time advancement for the nonlinear terms is a third-order Runge–Kutta (RK3) method. The second-order accurate Crank–Nicolson (CN) method is used for the linear terms.

We designed a distributed two-dimensional controller in two steps. First, we designed reduced-order controllers for two-dimensional Poiseuille flow in a periodic channel of streamwise length $L_x=4\pi$ at $\mathrm{Re}=5000$, which has the same mean wall-shear stress as turbulent channel flow at $\mathrm{Re}_\tau=100$. Subsequently, we fine-tuned the single-wave number reduced-order controllers in order to minimize the magnitude of the Fourier coefficients of the wall-shear stresses in turbulent channel flow at $\mathrm{Re}_\tau=100$. We used $N=32$ and $M=60$ in this linear model flow. Controllers operate at both top and bottom walls in parallel. If the two-dimensional controllers without model reduction were applied at each z

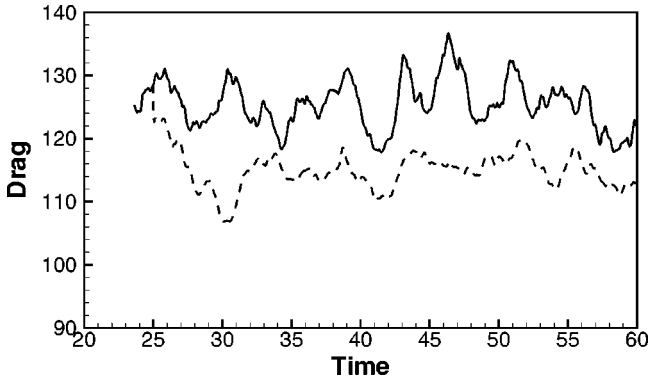

FIG. 2. Time history of the drag for the controlled and uncontrolled flows: – – –, controlled flow; ———, uncontrolled flow.

plane, then the order of the ensemble of controllers would be $64\times 3904=249\,856$. Using the model reduction technique previously described, we designed eight single-wave number controllers of order 12, corresponding to the eight lowest wave numbers. Since we use the eight lowest single-wave number controllers in our simulation, the combined order of the controllers is $64\times 96=6144$. It represents a state-space reduction of about 97.5%, with respect to the full-order system.

Figure 2 shows the time history of the drag in the uncontrolled and controlled flows. Drag is measured by the mean value of the wall-shear stresses averaged over each top and bottom wall. This two-dimensional control yields about a 10% drag reduction. Choi *et al.*[4] reported that the in-phase u control measured at $y^+=10$ also gives a 10% drag reduction. This in-phase streamwise velocity at the wall causes a similar effect, $du'/dy|_w\simeq 0$, which is the to-be-minimized target of our cost criterion in our two-dimensional controller. Note that this observed drag reduction is a byproduct since our controller is designed to suppress the fluctuations of the streamwise wall-shear stress, not the mean wall-shear stress. Note also the sudden drop in the drag as soon as the controller is switched on at $t=25$. This transient phenomena is also observed in other studies.[8,9]

Figure 3 compares the magnitude of Fourier coefficients of the wall-shear stresses in the controlled and uncontrolled flows. The wall-shear stresses are measured at the bottom wall at a given spanwise location. Figures 3(a) and 3(b) show the comparisons corresponding to wave numbers $k_x=0.5$ and $k_x=1.0$, respectively. Both figures show an order-of-magnitude reduction between the controlled and uncontrolled cases. The magnitude of the Fourier coefficients of wall-shear stress decreases very quickly as soon as the controller is activated at $t=25$. These results indicate that our distributed two-dimensional linear reduced-order controller suppresses disturbance wall-shear stress remarkably well, even in a fully developed turbulent flow. The high wave number components of the wall-shear stress in Fig. 3(c) do not show any reduction since only the lowest eight single-wave number controllers (up to $k_x=4.0$) are used in the control of flow. Examinations of other spanwise locations show similar results.

Contours of the disturbance wall-shear stresses at the bottom wall in the controlled and uncontrolled flows at $t=30$ are shown in Fig. 4. Contours for the uncontrolled flow show the usual elongated regions of low- and high-shear stress. Note that contours for the controlled flow show the dramatic effect of the distributed two-dimensional controller. The long streaky wall-shear stress region spans almost the entire streamwise direction, indicating that the low wave number components (except the zero wave number that we do not control) are completely suppressed, which is consistent with Fig. 3. The remaining spanwise variations, i.e., the alternating regions of high- and low-shear stress, are due to

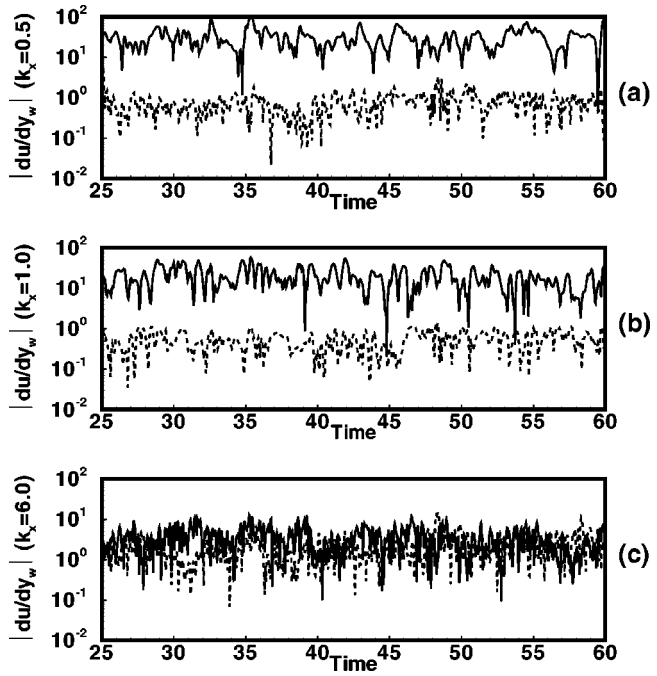

FIG. 3. Time history of the magnitude of the Fourier coefficients of the wall-shear stresses measured at the bottom wall at a given spanwise location for the controlled and uncontrolled flows: ———, uncontrolled flow; – – –, controlled flow. (a) $k_x=0.5$, (b) $k_x=1.0$, and (c) $k_x=6.0$.

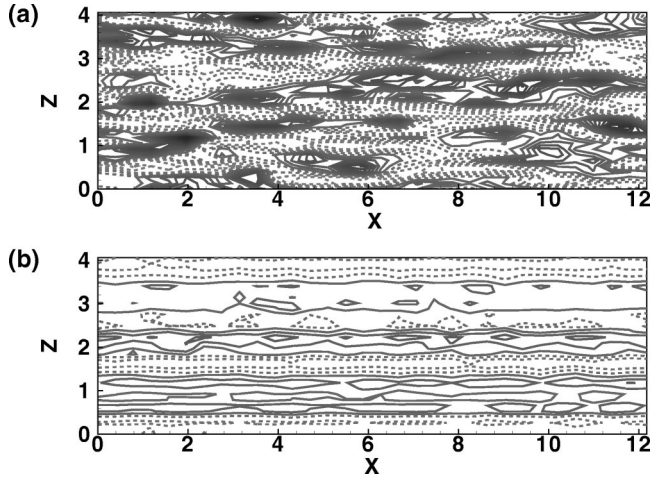

FIG. 4. Contours of disturbance wall-shear stresses at the bottom wall at $t=30$: (a) uncontrolled flow; (b) 2-D-controlled flow. Negative contours are dashed.

the fact that the two-dimensional controllers distributed along the streamwise direction are operated independently from one z plane to another.

The above results demonstrate that our distributed two-dimensional controller designed from the linear model works remarkably well in suppressing near-wall disturbances in the fully developed turbulent flow. The reduction of fluctuating wall-shear stress led to drag reduction. However, this distributed two-dimensional controller has a limited impact on the total drag since it cannot control the spanwise variation of the wall-shear stress. In the next section an augmentation to the distributed two-dimensional controller is presented and implemented.

V. AUGMENTED THREE-DIMENSIONAL CONTROLLER

In the previous section, successful control of fully developed turbulent channel flow has been obtained by applying a distributed two-dimensional controller. However, it has been observed that this controller does not account for the spanwise variations of fluid motion. An augmentation to the distributed two-dimensional controller that accommodates the three-dimensional characteristics of a fully developed turbulent flow is developed in this section.

A simple *ad hoc* control augmentation scheme is introduced in an attempt to capture the remaining spanwise variations of the controlled flow. This additional control, which generates blowing/suction to attenuate the spanwise variation of the wall-shear stress, is given as follows:

$$v_{\mathrm{ad}}(z)=C\left(\left.\frac{\partial u}{\partial y}\right|_w^{(x,z)}-\left.\frac{\partial u}{\partial y}\right|_w^{x}\right), \tag{27}$$

where $\partial u/\partial y|_w^{(x,z)}$ and $\partial u/\partial y|_w^{x}$ are the streamwise velocity gradients averaged over the xz plane and the x direction, respectively, and C is a constant to be adjusted for the best performance. The subscript ad indicates the *ad hoc* control, and v_{ad} is a function of only z. Therefore, the new control input is defined by

$$v_w(x,z)=v_{\mathrm{ad}}+v_{\text{2-D}}, \tag{28}$$

where $v_{\text{2-D}}$ is the actuation velocity generated by the distributed two-dimensional controller used in the previous section.

Using the distributed two-dimensional controller augmented with this *ad hoc* control scheme, the control of the fully developed turbulent flow with $\mathrm{Re}_\tau=100$ increased drag reduction to about 17%, as shown in Fig. 5. As before, the turbulent flow is left free to evolve without any wall actuation until $t=25$. As soon as the controller is activated at $t=25$, the drag drops sharply within a very small time period. The constant, C, in Eq. (27) is adjusted such that the root-mean-square (rms) value of the actuation is maintained at $0.1u_\tau$, where u_τ is the wall-shear velocity for the uncontrolled flow. We have found empirically that C between $0.05u_\tau$ and $0.2u_\tau$ gives a similar performance. An introduction of this simple control augmentation enhances the drag reduction, indicating that more sophisticated controllers that best take into account the three-dimensionality of turbulent flow may produce even more efficient suppression of skin-friction drag.

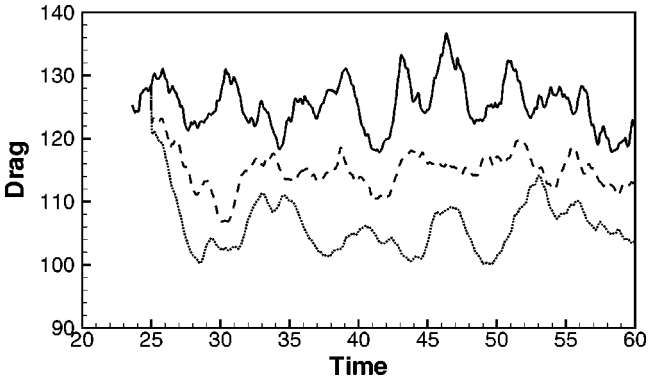

FIG. 5. Time history of the drag for the controlled and uncontrolled flows: ———, uncontrolled flow; – – –, 2-D-controlled flow; ···, *ad hoc*-controlled flow.

Figure 6 presents the comparison of contours of the disturbance wall-shear stresses at the bottom wall between the *ad hoc* controlled flow and the uncontrolled flow at $t=30$. Compared to Fig. 4, additional effort in the spanwise direction, v_{ad}, removes the pronounced peak–valley variation of the wall-shear stress that is observed in the controlled flow with the distributed two-dimensional controllers [see Fig. 4(b)]. Note that the high wave number components of the wall-shear stress are persistently sustained because of the lowest eight single-wave number controllers adopted in the control of flow.

VI. TURBULENCE STATISTICS

Some turbulence statistics of the flow field associated with the two controllers applied in this paper were examined to investigate the effect of the controllers on turbulence. All statistical quantities were averaged over a sufficiently long interval of time as well as over the planes parallel to the wall. For simplicity, the flows controlled by the distributed two-dimensional controller only and the distributed two-

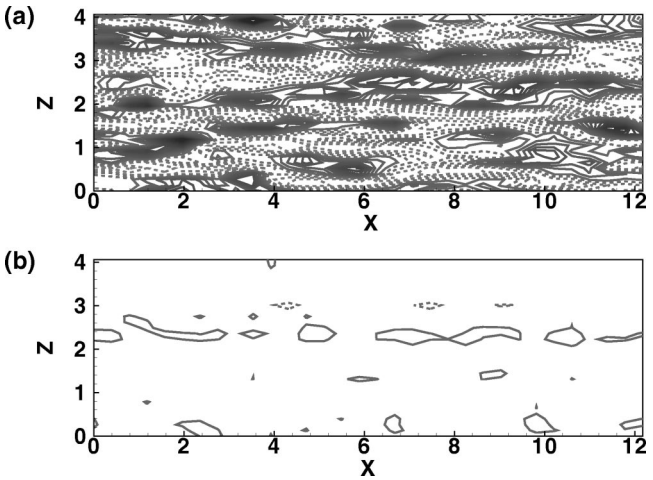

FIG. 6. Contours of disturbance wall-shear stresses at the bottom wall at $t=30$: (a) uncontrolled flow; (b) *ad hoc*-controlled flow. Negative contours are dashed.

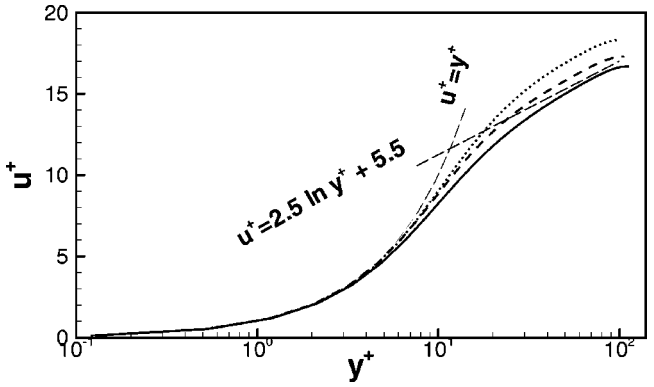

FIG. 7. Mean-velocity profiles: ···, *ad hoc*-controlled flow; – – –, 2-D-controlled flow; ———, uncontrolled flow.

dimensional controller augmented with the *ad hoc* control scheme are called ''2-D-controlled'' and ''*ad hoc*-controlled'' flows, respectively.

The mean velocity profiles normalized by the actual wall-shear velocities are shown in Fig. 7 for three different channel flows. These profiles show the same trend shown in the Choi *et al.*[4] drag-reduced flow: the slope of the log law for controlled flows remains the same while the mean velocity itself is shifted upward in the log-law region.

The root-mean-square (rms) values of turbulent velocity fluctuations are shown in Fig. 8 and compared to those of the uncontrolled flow. Note that all quantities in this figure are normalized by the wall-shear velocity of the uncontrolled flow. The controllers reduce the value of turbulent intensity significantly throughout the channel, especially for the wall–normal and spanwise components. The reduction of these quantities in the *ad hoc*-controlled flow is greater than that in the 2-D-controlled flow. The increase in v_{rms} very near the wall is due to the control input. A similar feature is also observed by Choi *et al.*[4] and Lee *et al.*[9] Both controllers mitigate the rms of spanwise velocity fluctuation throughout the channel compared to that in uncontrolled flow. However, the introduction of v_{ad} in Eq. (27) causes this value to increase very close to the wall, which also leads to an increase in the streamwise vorticity at the wall.

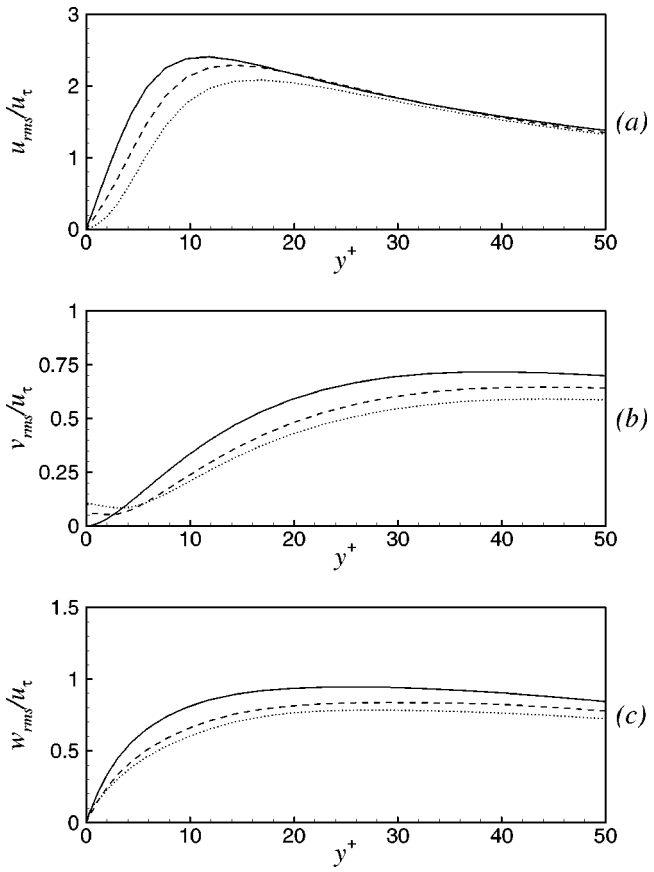

FIG. 8. Root-mean-square values of turbulent velocity fluctuations normalized by the wall-shear velocity, u_τ for the uncontrolled flow: ———, uncontrolled flow; – – –, 2-D-controlled flow; ···, *ad hoc*-controlled flow.

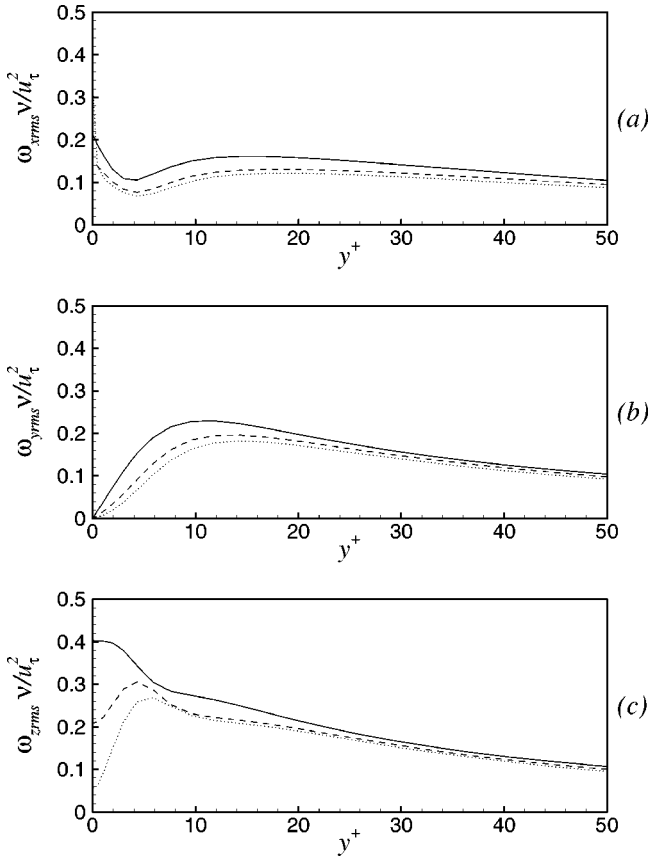

FIG. 9. Root-mean-square values of vorticity fluctuations normalized by the wall-shear velocity in wall coordinates: ———, uncontrolled flow; – – –, 2-D-controlled flow; ···, *ad hoc*-controlled flow.

Root-mean-square values of vorticity fluctuations for the controlled flows are compared with those for the uncontrolled flow in Fig. 9. All components of vorticity fluctuations are significantly reduced throughout the channel. Very close to the wall, however, the increase of streamwise vorticity in the *ad hoc*-controlled flow is due to the streamwise vorticity built at the wall by the *ad hoc* controller. The high streamwise vorticity at the wall slows the sweeping motion of high-momentum fluid induced by the streamwise vorticity away from the wall, thus resulting in a significant reduction in skin friction. A similar feature is also observed in Lee *et al.*[9] Note that the streamwise vorticity at the wall for the 2-D-controlled flow, however, is less than that for the uncon-

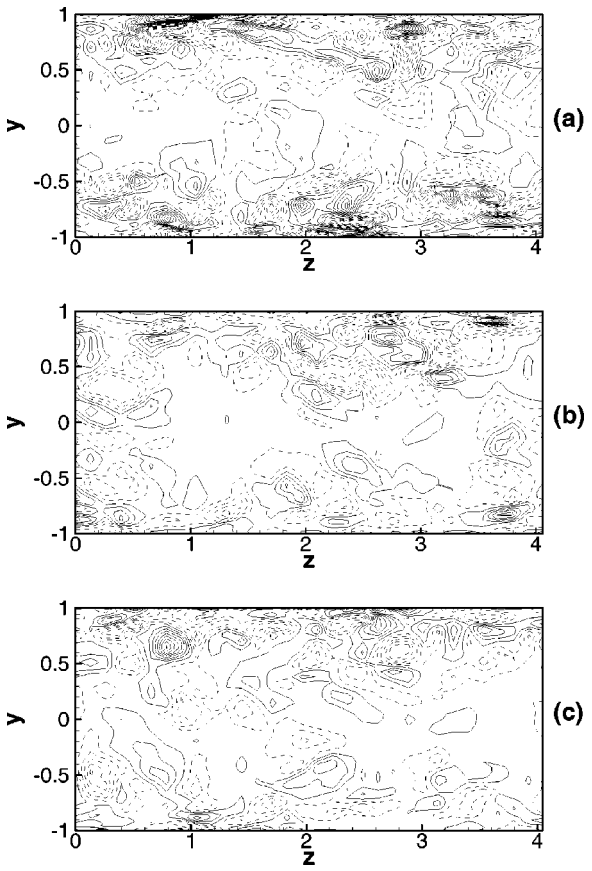

FIG. 10. A comparison of streamwise vorticity contours in a yz plane between controlled and uncontrolled flows: (a) uncontrolled flow; (b) 2-D-controlled flow; (c) *ad hoc*-controlled flow. Negative contours are dashed.

trolled flow. The reduction of ω_z is a direct consequence of the controller, which was designed to reduce $\partial u'/\partial y|_w$. The reduction of ω_y also indicates that our controllers weaken the strength of near-wall streaks. This also decreases the streak instability, which is shown to be responsible for regenerating the near-wall streamwise vortices.[29,30]

Figure 10 compares the streamwise vorticity fields in the uncontrolled and controlled flows. The strength of the near-wall streamwise vorticity for the controlled flows are greatly attenuated due to the wall transpiration produced by the controllers. It is discernible that the *ad hoc* controller diminishes the streamwise vorticity substantially more. The reduction of the strength of the streamwise vorticity has also been observed by Lee *et al.*[9] While Lee *et al.*[9] suppressed the streamwise vorticity field with the physical understanding that the control based on the weighted sum of $\partial w/\partial y|_w$ can prevent the physical eruption at the wall, the present controllers attenuate the streamwise vorticity strength by minimizing the streamwise disturbance wall-shear stress systematically. The present results further support the notion that a successful attenuation of the near-wall streamwise vortices results in a significant reduction in skin-friction drag.[4]

VII. CONCLUSIONS

A reduced-order linear feedback control based on a distributed two-dimensional controller design is applied to a turbulent channel flow. A controller based on a reduced model of the linearized Navier–Stokes equations for a laminar Poiseuille flow was designed by using LQG ($\mathcal{H}_2$)/LTR synthesis. This controller was implemented using input measurements that are the gradients of the streamwise disturbance velocity and output controls that are the blowing and suction at the wall.

First, we applied the distributed two-dimensional controller to both walls of a turbulent channel flow at $\mathrm{Re}_\tau = 100$. Eight single-wave number controllers corresponding to eight lowest wave numbers, reducing the order of the controller about 2.5% of the order of the full size system, are applied to attain a skin-friction reduction of 10% with respect to the uncontrolled turbulent flow. Next, a simple *ad hoc* augmented control scheme of the distributed two-dimensional controller is introduced to capture the three-dimensionality of turbulent flow. The control of fully developed turbulent flow by the distributed two-dimensional controller augmented by the *ad hoc* control scheme produces a 17% reduction in skin-friction drag. Motivated by this result, we are currently developing controllers to more efficiently account for the three-dimensionality of turbulent flow.

It should be noted that the present controller, which is based on a reduced-order linear system, has achieved its design objective, i.e., minimization of the wall-shear stress disturbances, quite remarkably when applied to the nonlinear flow. It was anticipated that the reduction of disturbances would also lead to a substantial reduction of the mean wall-shear stress. Unfortunately, this turned out not to be the case, suggesting that some other cost functions should be explored. By comparing with our previous results,[9,31] it was found that the present controller is not as effective in diminishing the strength of the streamwise vortices in the buffer layer, which was the primary target for other controllers, but achieved its design goal by mainly affecting the region very close to the wall. In this regard, minimization of the total disturbance energy in the flow field[32] or minimization of the linear coupling term[24] appears to be a good candidate to be explored. Whether either of these cost criterion is indeed controllable in nonlinear flows, however, remains to be investigated.

This study is carried out at low Reynolds number. Whether our controller, based on the reduced-order linear model, would work in other turbulent flows, should be drawn from real experiments or simulations at high Reynolds number. However, we expect that it should work equally well for high Reynolds number flow since our controller, derived from LQG/LTR synthesis, recovers the robustness of LQR, whose characteristics have been partially tested over the different Reynolds number flows.[33]

The statistics of controlled and uncontrolled flows are compared. The mean velocity profile is shifted upward in the log region, a typical characteristic of drag-reduced flow. Velocity and vorticity fluctuations as well as Reynolds shear stress (not shown) are significantly reduced due to the blowing/suction generated by the controller. However, a major change is confined to the wall region. Instantaneous flow fields show that the distributed two-dimensional controller

attenuates and modifies the streaky structure of the boundary layer. Streaks are observed to span the entire streamwise direction with velocity variations in the spanwise direction. These variations are substantially reduced by the augmented controller.

The three-dimensional aspect of the distributed two-dimensional controller by the augmentation of the *ad hoc* control further reduced the skin-friction drag. This three-dimensional controller produces secondary streamwise vorticity at the wall, which slows the sweeping motions of high-momentum fluid induced by the streamwise vorticity away from the wall. This induced retarding of the primary streamwise vorticity leads to additional drag reduction, which was also observed in Choi *et al.*[4]

Regarding the scaling factor C in Eq. (27), we found an optimal value of C that yields the blowing/suction of $0.1u_\tau$. With this optimal C, the augmented controller generates wall transpiration with a rms value of about $0.12u_\tau$. The required power input per unit area to the system, $p_w v_w + 0.5\rho v_w^3 \approx 0.1\rho u_\tau^3$, is significantly less than the power saved from the drag reduction, $\Delta C_f/C_f \dot{\tau}_w U_c \approx 3.2\rho u_\tau^3$, where p_w, ρ, C_f, τ_w, and U_c are the wall pressure, density, skin-friction coefficient, averaged wall-shear stress, and the centerline velocity, respectively.

Although the present two-dimensional controller augmented by an *ad hoc* three-dimensional controller has shown a promising result, it is apparent that we need to develop a three-dimensional controller using the same formulation presented in this paper. Extensions of LQG($\mathcal{H}_2$)/LTR design by using three-dimensional channel flow models are in progress.[34,35]

ACKNOWLEDGMENTS

We thank Dr. S. Joshi and Professor R. T. McCloskey for the enlightening discussions during the course of this work. We also thank V. Ryder and Sungmoon Kang for their proofreading.

This work is supported by AFOSR Grant No. F49620-97-1-0276 and by NASA Grant No. NCC 2-374 Pr 41.

[1] M. Gad-el-Hak, ''Interactive control of turbulent boundary layers—A futuristic overview,'' AIAA J. **32**, 1753 (1994).
[2] V. J. Modi, ''Moving surface boundary-layer control: A review,'' J. Fluids Struct. **11**, 627 (1997).
[3] H. L. Reed, W. S. Saric, and D. Arnal, ''Linear stability theory applied to boundary layers,'' Annu. Rev. Fluid Mech. **28**, 389 (1996).
[4] H. Choi, P. Moin, and J. Kim, ''Active turbulence control for drag reduction in wall-bounded flows,'' J. Fluid Mech. **262**, 75 (1994).
[5] R. Akhavan, W. J. Jung, and N. Mangiavacchi, ''Turbulence control in wall-bounded flows by spanwise oscillations,'' Appl. Sci. Res. **51**, 299 (1993).
[6] T. Berger, C. Lee, J. Kim, and J. Lim, ''Turbulent boundary layer control utilizing the Lorentz force,'' Phys. Fluids **12**, 631 (2000).
[7] H. Choi, R. Temam, P. Moin, and J. Kim, ''Feedback control for unsteady flow and its application to the stochastic Burgers equation,'' J. Fluid Mech. **253**, 509 (1993).
[8] T. Bewley and P. Moin, ''Optimal control of turbulent channel flow,'' ASME Conference, ASME DE-Vol. 75, 1994.
[9] C. Lee, J. Kim, D. Babcock, and R. Goodman, ''Application of neural networks to turbulence control for drag reduction,'' Phys. Fluids **9**, 1740 (1997).
[10] P. Koumoutsakos, ''Vorticity flux control for a turbulent channel flow,'' Phys. Fluids **11**, 248 (1999).
[11] S. Joshi, J. L. Speyer, and J. Kim, *Proceedings of the 34th Conference on Decision and Control*, New Orleans, Louisiana, December 1995.
[12] S. Joshi, J. L. Speyer, and J. Kim, ''A systems theory approach to the feedback stabilization of infinitesimal and finite-amplitude disturbances in plane Poiseuille flow,'' J. Fluid Mech. **332**, 157 (1997).
[13] S. Joshi, J. L. Speyer, and J. Kim, ''Finite dimensional optimal control of Poiseuille flow,'' J. Guid. Control Dyn. **22**, 340 (1999).
[14] T. Bewley and S. Liu, ''Optimal and robust control and estimation of linear paths to transition,'' J. Fluid Mech. **365**, 305 (1998).
[15] L. Cortelezzi and J. L. Speyer, ''Robust reduced-order controller of laminar boundary layer transitions,'' Phys. Rev. E **58**, 1906 (1998).
[16] L. Cortelezzi, K. H. Lee, J. Kim, and J. L. Speyer, ''Skin-friction drag reduction via robust reduced-order linear feedback control,'' Int. J. Comput. Fluid Dyn. **11**, 79 (1998).
[17] L. Cortelezzi, K. H. Lee, J. L. Speyer, and J. Kim, ''Robust reduced-order control of turbulent channel flows via distributed sensors and actuators,'' in *Proceedings of the 37th Conference on Decision and Control*, Tampa, Florida, December 1998.
[18] K. Zhou, J. C. Doyle, and K. Glover, *Robust and Optimal Control* (Prentice–Hall, Englewood Cliffs, NJ, 1996).
[19] I. Rhee and J. L. Speyer, ''A game theoretic approach to a finite time disturbance attenuation problem,'' IEEE Trans. Autom. Control **36**, 1021 (1991).
[20] A. E. Bryson and Y. C. Ho, *Applied Optimal Control* (Wiley, New York, 1969).
[21] H. Kwakernaak and R. Sivan, *Linear Optimal Control Systems* (Wiley Interscience, New York, 1972).
[22] J. C. Doyle and G. Stein, ''Multivariable feedback design: Concepts for a classical/modern synthesis,'' IEEE Trans. Autom. Control **AC-26**, 4 (1981).
[23] B. F. Farrel and P. J. Ioannou, ''Stochastic forcing of the linearized Navier–Stokes equations,'' Phys. Fluids A **4**, 1637 (1992).
[24] J. Kim and J. Lim, ''A linear process in wall-bounded turbulent shear flows,'' Phys. Fluids **12**, 1740 (2000).
[25] A referee pointed out that the wave number decoupling of this control problem was also recognized by others. See, for example, Bewley and Liu (Ref. 14) and Bewley and Agarwal in *CTR Proceedings of the 1996 Summer Program*, Stanford University, December 1996.
[26] C. M. Ho and Y. C. Tai, ''Microelectro-mechanical-systems (MEMS) and fluid flows,'' J. Fluids Eng. **118**, 437 (1996).
[27] B. Bamieh, F. Paganini, and M. A. Dahleh, ''Distributed control of spatially invariant systems,'' to appear in IEEE Trans. Automatic Control.
[28] J. Kim, P. Moin, and R. Moser, ''Turbulence statistics in fully-developed channel flow at low Reynolds number,'' J. Fluid Mech. **177**, 133 (1987).
[29] J. M. Hamilton, J. Kim, and F. Waleffe, ''Regeneration mechanisms of near-wall turbulence structures,'' J. Fluid Mech. **287**, 317 (1995).
[30] W. Schoppa and F. Hussain, ''A large-scale control strategy for drag reduction in turbulent boundary layers,'' Phys. Fluids **10**, 1049 (1998).
[31] C. Lee, J. Kim, and H. Choi, ''Suboptimal control of turbulent channel flow for drag reduction,'' J. Fluid Mech. **401**, 245 (1998).
[32] P. Moin and T. Bewley, ''Application of control theory to turbulence,'' *12th Australian Fluid Mechanics Conference*, Sydney, Australia, 10–15 December 1995.
[33] K. H. Lee, ''A system theory approach to control of transitional and turbulent flows,'' Ph.D. dissertation, Department of Mechanical Engineering, University of California, Los Angeles, CA, September 1999.
[34] S. M. Kang, V. Ryder, L. Cortelezzi, and J. L. Speyer, ''State-space formulation and control design for three-dimensional channel flows,'' *1999 American Control Conference*, San Diego, California, 2–4 June 1999.
[35] S. M. Kang, L. Cortelezzi, and J. L. Speyer, ''Performance of a linear controller for laminar boundary layer transition in three dimensional channel flow,'' in *Proceedings of the 38th Conference on Decision and Control*, Phoenix, Arizona, 7–10 Dec. 1999.